

# Dual-wavelength Humidity Profiles using S-PolKa During the DYNAMO Field Campaign

S.M. Ellis\*, J. Vivekanandan  
National Center for Atmospheric Research, Boulder CO

## 1. Introduction

The NCAR scanning, S- and  $K_a$ -band dual-wavelength, dual-polarimetric, radar (S-PolKa) makes simultaneous S-band and  $K_a$ -band measurements with  $1^\circ$  beamwidth and nominal range resolution of 150 m. Both radars have dual-polarization and Doppler measurement capabilities. The S-PolKa radar is a national resource as part of the NSF Deployment Pool and has been deployed for atmospheric studies around the world. The dual-wavelength and dual-polarization capabilities of S-PolKa enable the estimation of humidity profiles in the lower troposphere (Ellis and Vivekanandan, 2010) and liquid water content (LWC). Using the LWC estimates and making some reasonable assumptions results in mass weighted diameter ( $D_0$ ) estimates (Ellis and Vivekanandan, 2011).

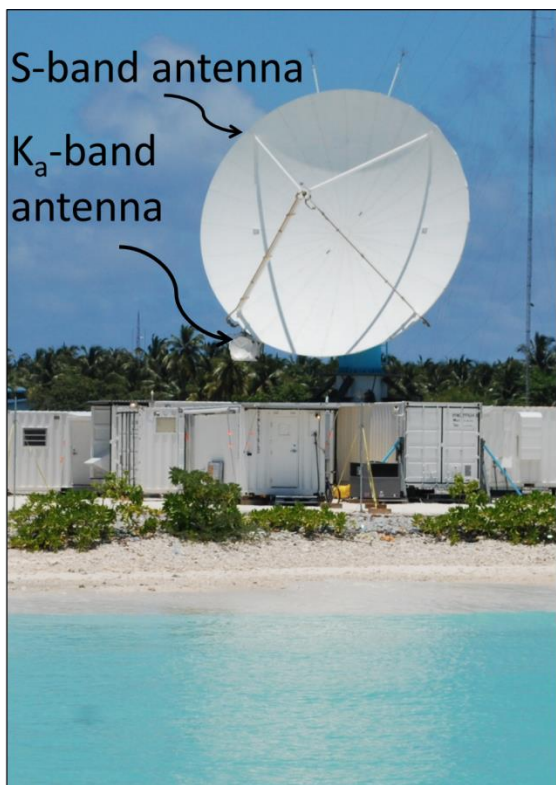


Fig 1. The S-PolKa radar deployed in the Maldives during DYNAMO.

\* Corresponding author address: Scott M. Ellis, National Center for Atmospheric Research, P.O. Box 3000, Boulder CO 80307; email: sellis@ucar.edu.

The simultaneous S- and  $K_a$ -band measurements are achieved by mounting the  $K_a$ -band antenna directly on the much larger S-band antenna, as shown in Fig. 1.

The S-PolKa system was deployed in the Maldives for 4.5 months during the Dynamics of the Madden Julian Oscillation (DYNAMO) field campaign (Yoneyama et al.2013). During DYNAMO, the real-time, automated Radar Estimated Profiles of Humidity (REPoH) algorithm operated, providing radar-based humidity profiles. This was the first deployment of REPoH, allowing the processing of large amounts of data.

The S-PolKa-retrieved humidity computed via REPoH is verified against nearby 3 hourly sounding data. Only radar and sounding data that were very close in time and space were used in order to minimize the impact of the natural variability and the sampling differences. The results showed the radar-based humidity was essentially unbiased in comparison to the sounding measurements.

The humidity retrievals typically measured large spatial and temporal variability. By measuring the spatial and temporal variability of the low-level humidity, a better representation of the mean environmental humidity values is obtained compared to a single profile. Further the radar-based retrievals can be used to examine how the low-level humidity varies on individual cases and in relation to the observed cloud systems. Preliminary data will be shown.

## 2. Humidity Retrieval

The dual-wavelength humidity retrieval of Ellis and Vivekanandan (2010) takes advantage of the characteristics of atmospheric attenuation at the different wavelengths. The  $K_a$ -band attenuation through the atmosphere is strongly dependent on the amount of water vapor present. The S-band atmospheric attenuation is several orders of magnitude less than at  $K_a$ -band and can be ignored. These principles are illustrated well by Lhermitte (1987) and reproduced here in Fig. 2, which shows the one-way atmospheric attenuation as a function of radar operating frequency for various water vapor content values. If the  $K_a$ -band atmospheric attenuation is known through a layer of the atmosphere, then the mean water vapor content of the layer can be determined.

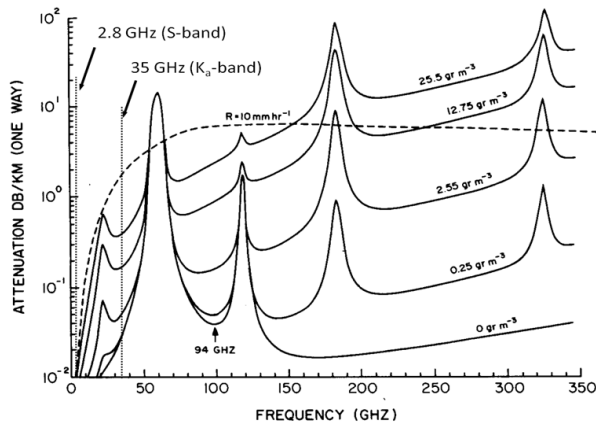


Fig 2. One-way atmospheric attenuation ( $\text{dB km}^{-1}$ ) plotted as a function of frequency (GHz) for different water vapor content values ( $\text{g m}^{-3}$ ) (from Lhermitte, 1987).

In order to estimate the atmospheric attenuation at  $K_a$ -band, the  $K_a$ -band reflectivity value is subtracted from the S-band reflectivity at the end of radar ray segments through cloud and precipitation free atmosphere. Primary ray segments start at the radar and end at the nearest edge of an echo as illustrated in Fig. 3. Ray segments can also start at the back edge of an echo and extend to the front edge of another echo further in range. These so-called secondary rays are possible far less frequently than primary ray segments.

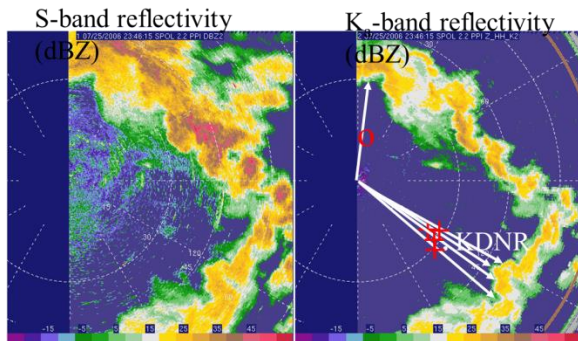


Fig. 3. Examples of possible ray segments for the dual-wavelength radar humidity retrievals.

The data used to form the ray segments must be from Rayleigh scatterers at both  $K_a$ - and S-band and the impact of measurement noise must be small compared to the attenuation. The procedures to ensure these requirements are met are described in detail in Ellis and Vivekanandan (2010). To summarize, the ray segments must be a minimum of 15 km in length and we average a minimum of 10 radar range gates in a 2-D patch at the front edge of the echoes.

The next step is to relate the estimated humidity to the water vapor content. To achieve this, a relation between atmospheric attenuation and water vapor content was developed using the microwave propagation model of Liebe (1985). The model was run numerous times varying the pressure, temperature and water vapor content over their natural ranges for the environment. The results are plotted as a function of water vapor content in Fig. 4. The + symbols in Fig. 4 represent the model results for various atmospheric states representing a tropical environment. The horizontal spread of the results is due to the small dependency of attenuation on temperature and pressure. The solid line is the best fit, 3<sup>rd</sup> degree polynomial for the simulations given by the equation below the curve. The dashed line is a similar best fit curve for simulations representing the environment in Colorado. The curve is different due to the higher altitude. To retrieve the water vapor content, the attenuation estimate is simply plugged into the appropriate equation shown in Fig. 4.

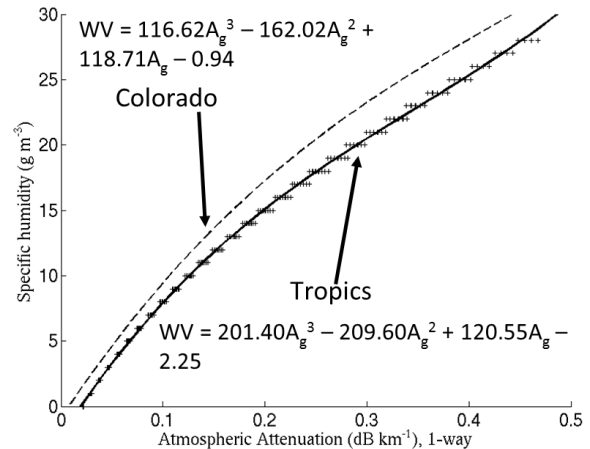


Fig. 4. The relationship of humidity to  $K_a$ -band atmospheric attenuation as derived from Liebe (1985).

Once the humidity is estimated, the value can be plotted at the height of the midpoint of the ray segment. The retrieval requires cloud/precipitation echoes to be present and is severely limited if there is heavy rain right over the radar.

### 3. S-PolKa at DYNAMO

The DYNAMO field campaign occurred in 2011 and 2012 in the Indian Ocean. DYNAMO was a large, multi-agency, international field campaign with numerous in-situ and remote sensing platforms including; ground-based, ship-borne and aircraft (Gottschalk et al., 2013). As part of DYNAMO, the NCAR S-PolKa radar was deployed on the Addu Atoll in the Maldives from 1 October, 2011 to 15 January, 2012. The radar was run with the same sequence of

plan position indicator (PPI) volume and numerous range height indicator (RHI) scans with a 15 minute schedule over the entire 4.5 months. The radar was run 24 hours a day, 7 days a week for the duration of the project. The REPoH algorithm was run in real-time, producing humidity retrievals throughout the project.

During DYNAMO the DOE launched 8 daily soundings on Addu Atoll approximately 8 km southeast of S-PolKa. This provided an excellent opportunity to compare the automated radar-based humidity retrievals from REPoH with the in-situ sounding data.

#### 4. Comparison of Radar-derived Humidity to Soundings

The dual-wavelength radar retrievals of humidity, or REPoH data, were compared to the nearby soundings over the 4.5 month period S-PolKa operated at DYNAMO. Due to the variability in the humidity observed by the soundings and the radar, it was important to include only REPoH data near the sounding in space and time. The region of comparison was limited to radar azimuths within  $2^\circ$  of the sounding site. The range limits were from 10 km to 20 km. Since the REPoH retrieval requires a minimum range, we could not match the location of the sounding in range. Finally, the radar-based humidity estimate had to be within 15 minutes of the sounding time. The geometry of the comparison zone is shown in Fig. 5.



Fig. 5. The Addu Atoll with the locations of the S-PolKa radar, DOE sounding site and a sketch of the region for radar humidity retrievals compared to the sounding (red shading).

The result was 44 points of comparison. The mean bias between the sounding and REPoH humidity was  $-0.14 \text{ g m}^{-3}$  and the root mean square

difference (RMSD) was  $1.57 \text{ g m}^{-3}$ . A scatter plot of sounding versus radar humidity is shown in Fig. 6. The points scatter along the 1-to-1 line (red solid line). The correlation of the REPoH retrievals to the sounding measured humidity is 0.79.

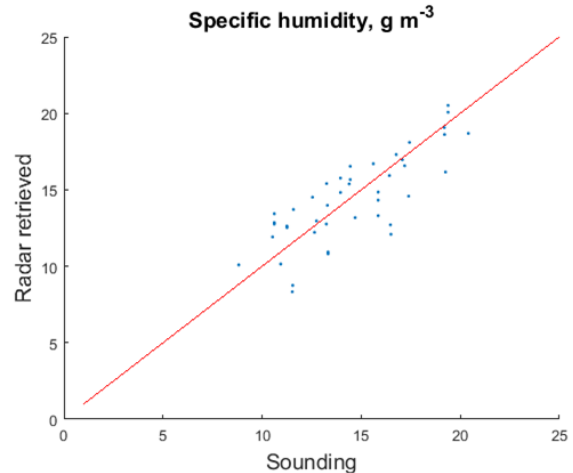


Fig. 6. Scatter plot of humidity ( $\text{g m}^{-3}$ ) measured by the DOE soundings versus radar-estimated humidity. The data are from the 4.5 months of data collected during DYNAMO.

The difference between the REPoH humidity and the sounding humidity is likely partly due to the differences in location and timing of the measurements. To test the sensitivity of the comparison to spatial constraints, we repeated the analysis successively relaxing the azimuth and range limits. The results, listed in Table 1, show that the RMSD and bias increase and the correlation decreases for increasingly large regions. Therefore the variability of the humidity during DYNAMO is an important factor to consider in the comparison of REPoH and sounding humidity.

Table 1. RMSD, bias, correlation coefficient and the number of points for experiments increasing the radar region compared to sounding humidity.

Data filter (Sounding site at azimuth = 140 deg, range = 8km)	RMSD	Bias	Corr	# point
138>az>142, 10> range>16	1.57	-0.14	0.79	44
130>az>150, 10> range>16	1.73	-0.26	0.75	276
130>az>150, 10> range>25	1.75	-0.54	0.74	517
110>az>170, 10> range>25	1.77	-0.17	0.68	1533
50>az>230, 10> range>25	1.86	0.03	0.62	3867
all az, all range	2.12	0.53	0.57	9878

#### 5. Humidity Variability Observed in DYNAMO

The humidity in the tropics has been observed to be highly variable in space and time (Davison et al. 2013). This was also true in the Indian Ocean during



DYNAMO. Dropsondes from the NOAA P-3 aircraft taken over a few minutes as the aircraft circled Addu Atoll illustrate the high spatial variability of humidity. Figure 7 shows 6 dropsonde humidity profiles taken on 8 November 2011 between 10:25 and 10:35 UTC all within about 20 km of Addu Atoll. The different colored lines indicate the general direction of the dropsonde from the S-PolKa radar. At a given height above the ocean the humidity can vary up to nearly  $5 \text{ g m}^{-3}$ . This is a very large change in humidity over a relatively small time interval and spatial extent. Under these conditions it is clear that a single sounding profile will not capture a humidity profile that is representative of the larger environment. This may cause problems for numerical models that cannot resolve small scale humidity variations and need to know the variability of the input humidity.

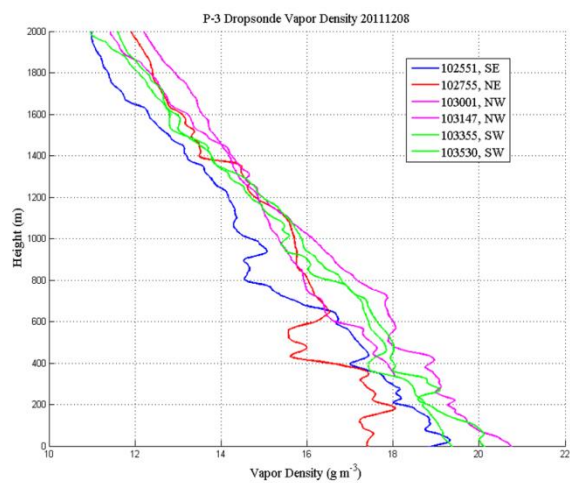


Fig. 7. NOAA P-3 dropsonde humidity profiles from sondes dropped in about a 20 km ring around S-PolKa over a 10 minute period.

As it was raining on the S-PolKa radar during the period of the dropsonde launches shown in Fig. 7, REPoH profiles were not possible. This illustrates one of the limitations of the radar method. Figure 8 shows the REPoH estimated humidity profiles for one hour of observations including all  $360^\circ$  of azimuth angles on 12 December, 2011 from 04:05 to 05:05 UTC. Each plus symbol in Fig. 8 represents the humidity over a single ray segment plotted at the height of the midpoint of the segment. It can be seen that the spread of the data at most levels is about  $3$  to  $5 \text{ g m}^{-3}$ , similar to the dropsonde data in Fig. 7. The mean humidity is illustrated as the black line in Fig. 8. This mean is a better representation of the mean environmental low-level humidity than a single profile from the radar or a sonde.

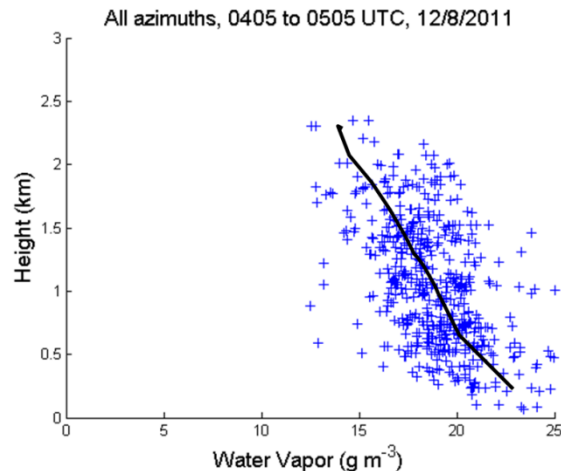


Fig. 8. Water vapor retrievals (blue +) from REPoH covering  $360^\circ$  azimuth from 04:05 to 05:05 UTC on 8 December, 2011. The black line represents the mean water vapor retrieved over the hour.

Next the REPoH retrievals shown in Fig. 8 were parsed into smaller time and space intervals in an arbitrary manner. The time was limited to 15 minute intervals, or one volume time, and the space was limited to  $45^\circ$  azimuth. The application of these arbitrary restrictions of time and space resulted in retrievals with much less variation and appear more like coherent profiles of humidity than including all of the data shown in Fig. 8. Three examples of the  $45^\circ$  azimuth and 15 minute REPoH retrievals are shown in Fig. 9. The individual profiles shown in Fig. 9 are coherent, but with different values, indicative of spatial variance of humidity during this hour. Thus the REPoH humidity estimates can characterize to some extent the spatial distribution of humidity.

## 6. Summary and Conclusions

The NCAR S-PolKa dual-wavelength, dual-polarimetric, Doppler research radar was deployed for 4.5 months on Addu Atoll in the central Indian Ocean during the DYNAMO field project. The REPoH automated real-time procedure to estimate the humidity following Ellis and Vivekanandan (2010) was run during the 24 hours, 7 days a week observations.

The results of the REPoH algorithm were compared to nearby soundings and found to have very little bias, high correlation and a reasonable RMSD compared to sounding humidity measurements.

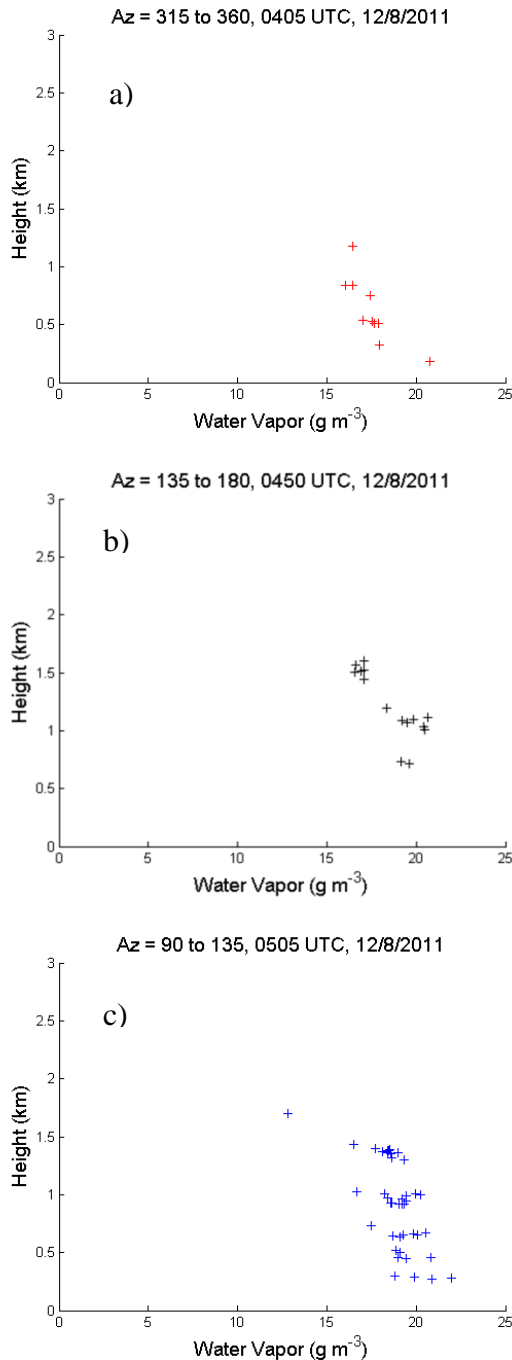


Fig. 9. The REPoH humidity from within the same hour of data shown in Fig. 8, but parsed into 15 minute time segments and  $45^\circ$  azimuth segments.

Further it was shown that the characterization of the high spatial and temporal variability of humidity in the tropics can be improved with the REPoH retrievals under the right circumstances. While dependent on the distribution of echoes and not available 100% of the time, the radar-based REPoH humidity profiles can often measure the humidity distribution and variability that can augment the sounding data. This

additional information provided by the radar-based humidity estimates may be incomplete, but it adds considerable knowledge of the distribution and variability of low-level humidity that would otherwise not be available.

### Acknowledgments

The National Center for Atmospheric Research is sponsored by the National Science Foundation. Any opinions, findings and conclusions or recommendations expressed in this publication are those of the author(s) and do not necessarily reflect the views of the National Science Foundation.

### 7. References

Davison, Jennifer L., Robert M. Rauber, Larry Di Girolamo, Margaret A. LeMone, 2013: A Revised Conceptual Model of the Tropical Marine Boundary Layer. Part I: Statistical Characterization of the Variability Inherent in the Wintertime Trade Wind Regime over the Western Tropical Atlantic *Journal of the Atmospheric Sciences*, **70**, Issue 10 pp. 3005-3024

Ellis, S. M. and J. Vivekanandan, 2010: Water Vapor Estimates Using Simultaneous Dual-wavelength Radar Observations. *Radio Sci.*, **45**, doi:10.1029/2009RS004280.

Gottschalck, Jon, Paul E. Roundy, Carl J. Schreck III, Augustin Vintzileos, and Chidong Zhang, 2013: Large-Scale Atmospheric and Oceanic Conditions during the 2011–12 DYNAMO Field Campaign. *Mon. Wea. Rev.*, **141**, 4173–4196. doi: <http://dx.doi.org/10.1175/MWR-D-13-00022.1>

Lhermitte, R., 1987: A 94-GHz Doppler Radar for Cloud Observations. *J. Atmos. Oceanic Technol.*, **4**, 36–48.

Yoneyama, K., C. Zhang, and C.N. Long, 2013: Tracking pulses of the Madden-Julian Oscillation. *Bull. Amer. Met. Soc.*, **94**, 1871-1891.